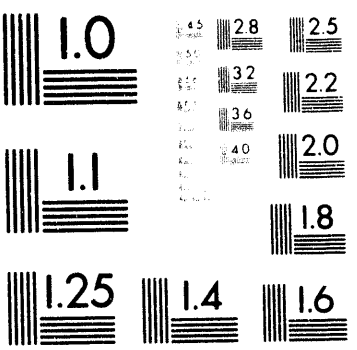
1.0
1.1
1.25
1.4
1.6
1.8
2.0
2.2
2.5
2.8
3.2
3.6
4.0
4.5

1 of 1

A-UR-93-2549

Conf-930713--24

os Alamos National Laboratory is operated by the University of California for the United States Department of Energy under contract W-7405-ENG-36

TITLE: SHOCK INITIATION STUDIES OF LOW DENSITY HMX USING ELECTROMAGNETIC PARTICLE VELOCITY AND PVDF STRESS GAUGES

AUTHOR(S): Stephen A. Sheffield, Richard L. Gustavsen, Robert R. Alcon - LANL, M-7

SUBMITTED TO: Tenth International Detonation Symposium, Boston, MA - July 12-16, 1993

DISCLAIMER

Los Alamos Los Alamos National Laboratory
Los Alamos, New Mexico 87545

FORM NO 836 R4
ST NO 2629 5/81

SHOCK INITIATION STUDIES OF LOW DENSITY HMX USING ELECTROMAGNETIC PARTICLE VELOCITY AND PVDF STRESS GAUGES

Stephen A. Sheffield, Richard L. Gustavsen, and Robert R. Alcon
Los Alamos National Laboratory
Los Alamos, New Mexico 87545

Robert A. Graham and Mark U. Anderson
Sandia National Laboratories
Albuquerque, NM 87185

Magnetic particle velocity and PVDF stress rate gauges have been used to measure the shock response of low density HMX (1.24 g/cm^3). In experiments done at LANL, magnetic particle velocity gauges were located on both sides of the explosive. In nearly identical experiments done at SNL, PVDF stress rate gauges were located at the same positions so both particle velocity and stress histories were obtained for a particular experimental condition. Unreacted Hugoniot data were obtained and an EOS was developed by combining methods used by Hayes, Sheffield and Mitchell (for describing the Hugoniot of HNS at various densities) with Hermann's P-α model. Using this technique, it is only neccesarry to know some thermodynamic constants or the Hugoniot of the initially solid material and the porous material sound speed to obtain accurate unreacted Hugoniots for the porous explosive. Loading and reaction paths were established in the stress-particle velocity plane for some experimental conditions. This information was used to determine a global reaction rate of $\sim 0.13\ \mu s^{-1}$ for porous HMX shocked to 0.8 GPa. At low input stresses the transmitted wave profiles had long rise times (up to 1 μs) due to the compaction processes.

INTRODUCTION

Porous octotetramethylene tetranitramine (HMX) at a density of 1.24 g/cm^3 has been shown to reproducibly undergo a deflagration-to-detonation transition (DDT) from small inputs when suitably confined.[1] This gives rise to safety concerns which is the principal reason for studying it under low shock input conditions.

Studies of low-density explosives (less than 80% of theoretical maximum density -- TMD) have been conducted on several explosive materials over the past 30 years. Seay and Seely[2] studied shock initiated low density PETN and showed that, at a density of 1.0 g/cm^3 (65% TMD), this material could be initiated with shock inputs as low as 0.25 GPa. Evans et al.,[3] made measurements on ammonium perchlorate at a density of 1.0 g/cm^3 (51% TMD) and found that shock inputs as low as 1.7 GPa would initiate it. Dremin et al.,[4] used magnetic gauges to study the initiation of bulk density TNT and tetryl charges. They found inputs of 1.1 GPa produced runs to detonation between 16 and 54 mm, depending on the TNT particle size. Lindstrom[5] did a rather large study on tetryl at densities of 1.3, 1.4, 1.5, 1.6, and 1.7 g/cm^3. At a density of 1.30 g/cm^3 (75% TMD) an input of 0.47 GPa gave a run distance to detonation of 10 mm.

Two studies with direct application to this work have been done on low density HMX. Dick performed several explosively driven cutback tests in which he measured the average transit time through HMX compacts of different thicknesses (at a density of 1.24 g/cm^3) for inputs of 0.8 and 2.1 GPa.[6] By plotting transit time vs. compact thickness, he was able obtain some Hugoniot and initiation information. He determined the distance to detonation was 3.0 mm for an input of 2.1 GPa and 5.2 mm for an input of 0.8 GPa. Elban and Chiarito subjected two different HMX powders to slow compactiou conditions up to 0.2 GPa.[7] They found that the breakage of HMX crystals starts at stresses below 1 MPa and that widespread crystal fracture takes place between 62 and 75% of TMD. At a stress of 0.2 GPa, 96% of TMD was obtained. The data from these studies are not sufficient

to construct a reliable equation of state (EOS) so we embarked upon a study to make time-resolved measurements as an extension of Dick's work with manganin gauges.[8]

Nearly all the previous experimenters have used explosive driver/attenuator systems to obtain the desired input shocks so the exact input shock amplitudes and shapes were not well known. In addition, many of them used diagnostics (such as measurement of shock breakout with a streak camera) which did not give detailed shock parameter histories. The samples were in the form of wedge or pellet shaped compacts, carefully pressed and shaped before assembly to the attenuator plate of the driver system. Only Dremin et al.,[4] made in-situ measurements of particle velocity histories in bulk density TNT; this allowed them to measure details of the reactive-wave growth process.

In our experiments magnetic particle velocity measurements were made at Los Alamos National Lab. (LANL) and polyvinylidene difluoride (PVDF) stress rate measurements[9,10] were done at Sandia National Labs. (SNL) in experiments that were nearly identical. Time resolved measurements of these two properties allows tracking of any process occurring (e.g. compaction or reaction) in the stress vs. particle velocity plane. In this paper we develop an EOS for low density HMX, discuss the experimental methods, the data obtained, and their interpretation.

EQUATION OF STATE

Equation of state information is difficult to obtain on porous explosives for several reasons. At low input stresses, compaction behavior dominates and transmitted waves become disperse. At higher inputs, because the materials are very sensitive to the shock initiation of detonation, reaction occurs and shock velocity information is not reliable, i.e., transit time measurements cannot be used. Even at pressures of only a few kbars, the explosive may start to react and accelerate the wave. In wedge tests, wave acceleration is often apparent well before the onset of detonation. Because of the dynamic compaction processes and early onset of reaction, measurements of pressure or particle velocity in transmitted waves provide unreliable EOS information as well. The best information has been obtained in flying plate experiments using flyers made of well characterized materials whose velocities were accurately measured and when pressure or particle velocity was measured at the flyer/explosive interface. Data from these types of experiments is uncommon, as most researchers have been more interested in the initiation properties, and have used wedge experiments.

Equations of state have been developed for porous explosive materials in the past.. Lindstrom[5] developed an EOS for tetryl. Erkman and Edwards[11] constructed an EOS form in which different parameter values could be used to describe the behavior of RDX, tetryl, PETN, and ammonium nitrate. Sheffield, Mitchell, and Hayes[12] used an EOS based on the Helmholtz potential and a Murnaghan isotherm to model HNS (hexanitrostilbene) shock behavior. We use the Helmholtz form as the basis for the EOS development in this paper.

Because of the difficulties in making reliable EOS measurements on porous explosives it is often useful to construct a Hugoniot using thermodynamic constants obtained from static and hydrostatic measurements, the bulk sound speed of the porous explosive, and then to properly account for the porosity. If hydrostatic data is unavailable, the thermodynamic constants can be obtained by fitting to Hugoniot measurements of explosives at near 100% TMD or on single crystals. These are generally much less sensitive to shock initiation.

Porous Explosive EOS

The formalism for the equation of state which is used in this paper was developed by Hayes, and was first used to describe the porous explosive, HNS by Sheffield, Mitchell and Hayes.[12] It was later ammended by Setchell and Taylor[13] to be used in Hermann's P-α model.[14] Thus, the ideas are not new, but neither have they seen widespread application.

The method is based on constructing a complete thermodynamic potential function for the fully dense explosive, namely the Helmholtz Free Energy. The specific form which Hayes chose for the Helmholtz Free Energy is[12]

$$F(T,V) = C_v\left[(T - T_0)\left(1 + \frac{\gamma}{V}(V_0 - V)\right) + T\ln\left(\frac{T_0}{T}\right)\right] + \frac{K_{T_0}V_0}{N(N-1)}\left[\left(\frac{V_0}{V}\right)^{N-1} - (N-1)\left(1 - \frac{V}{V_0}\right) - 1\right] \quad (1)$$

where C_v is the specific heat at constant volume, γ is Gruneisen's parameter, V_0 is the specific volume of the

fully dense explosive at zero pressure, K_T is the bulk modulus at constant temperature, and N is a constant. This construction assumes C_v and γ/V are constants, while the bulk modulus is

$$K_T = K_{T_0}\left(\frac{V_0}{V}\right)^N. \qquad (2)$$

These constants are readily obtained from static thermodynamic measurements and hydrostatic pressure-volume measurements.

In order to describe the compaction of the porous explosive in the framework of Hermann's P-α model,[14] Eq. (1) must be recast in the form $P(E,V)$ or $E(P,V)$. Setchell and Taylor[13] have shown that

$$\begin{aligned} E(P,V) = {} & \frac{P}{\gamma/V} - \frac{\gamma}{V} C_v T_0 (V_0 - V) \\ & - \frac{K_{T_0}}{N\gamma/V}\left[\left(\frac{V_0}{V}\right)^N - 1\right] \\ & + \frac{K_{T_0} V_0}{N(N-1)}\left[\left(\frac{V}{V_0}\right)^{1-N} \right. \\ & \left. - (N-1)\left(1 - \frac{V}{V_0}\right) - 1\right] \end{aligned} \qquad (3)$$

Eq. (3) describes the behaviour of the fully dense explosive. While Eq. (1) is a complete thermodynamic EOS, Eq. (3) is not.

Hermann's theory,[14] as modified by Carroll and Holt[15] states that in a porous material, Eq. (3) describes the solid portion. The distension of the porous material is

$$\alpha = V/V_s, \qquad (4)$$

where V is the specific volume of the porous explosive at a given pressure and energy, and V_s is the specific volume of the solid explosive at the same pressure and energy. If in the porous material the average pressure is P and the average specific volume V, then the pressure in the solid portion is $P\alpha$ and the specific volume of the solid portion is V/α. Equation (3) can thus be used to describe the energy at average pressure P and volume V in the porous explosive if modified to describe only the solid portion:

$$E = E(P\alpha, V/\alpha). \qquad (5)$$

Eqs. (3), (4), and (5) are now augmented by defining α as a function of the shock pressure P. A simple form for $\alpha(P)$, such as the following one suggested by Herman,[14] is sufficient.

$$\begin{aligned} \alpha &= 1 + (\alpha_0 - 1)(1 - P/P_s)^2 \quad (P \le P_s) \\ \alpha &= 1 \qquad\qquad\qquad\qquad (P \ge P_s) \end{aligned} \qquad (6)$$

In Eq. (6), α_0 is the original distension, $\alpha_0 = V_{00}/V_0$, and V_{00} is the initial specific volume of the porous explosive. P_s is the pressure at which the material crushes to solid density. Herman has also shown how P_s can be determined from measurements of the sound speed in the porous material.[14] Different values of P_s must be used for different initial porosities.

Given P and $\alpha(P)$, Eq. (5) is then itteratively solved for V such that the energy is the same as that given by the Hugoniot jump condition $E = P/2(V_{00} - V)$. Given the quality of much of the experimental EOS data, further sophistication in an EOS is unwarranted. Constants used in the EOS analysis will be discussed later when the HMX Hugoniot data are presented.

EXPERIMENTAL DETAILS

Experiments at both labs utilized gas gun driven projectiles to obtain sustained-shock input conditions. Projectile velocities were nearly the same at both labs for a given experimental setup so that in separate, similar experiments, both stress and particle-velocity histories were measured.

HMX powder was confined in sample cells which had a polychlorotrifluoroethylene (Kel-F) front face (on which the projectile impacted) and a poly 4-methyl-1-pentene (TPX) cylindrical plug back. (TPX is a low impedance material and therefore a reasonable impedance match to the pressed HMX.) Gauges were epoxied on the HMX side of both pieces. The front face was screwed to a Kel-F confining cylinder with an outside diameter of 68.6 mm and an inside diameter of 40.6 mm. The pressed HMX (between the Kel-F and TPX) was ~ 4 mm thick and had a density of 1.24 g/cm^3. Figure 1 is a cross-section ot the cylindrical experimental setup showing the various parts.

The HMX powder used in all the experiments was coarse HMX from Holston (Lot HOL 920-32) with a bulk density of ~ 1.16 g/cm^3 (see Ref. 6). The material was screened to eliminate agglomerates and a few of the largest particles.

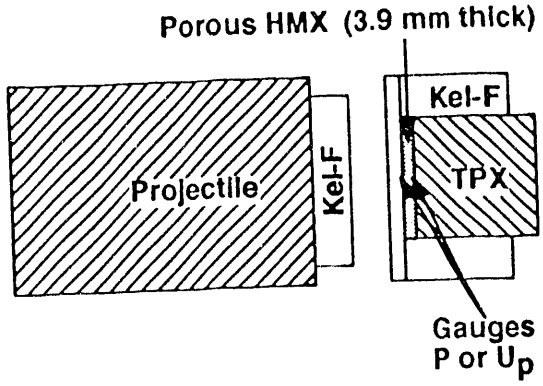

FIGURE 1. CROSS SECTION OF EXPERIMENTAL SETUP.

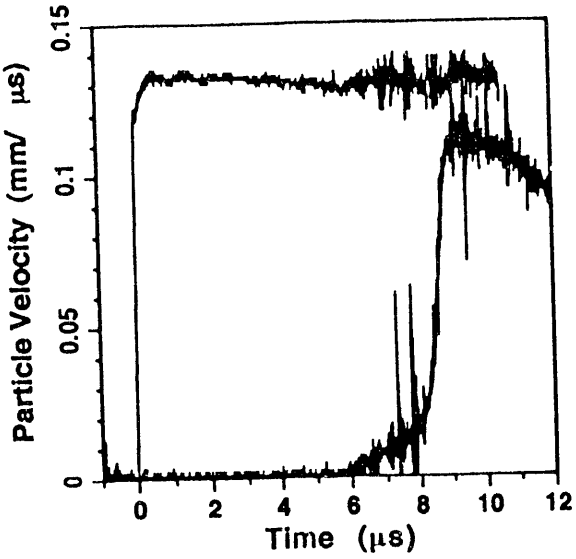

FIGURE 2. PARTICLE VELOCITY WAVEFORMS FOR SHOT 931.

In the LANL experiments the magnetic particle-velocity gauges were 25 μ thick FEP Teflon with a 5 μ thick aluminum "stirrup" gauge on it. Active region of the gauge was 10 mm by 0.5 mm. In the SNL experiments PVDF stress-rate gauges were composed of 25 μ thick PVDF with plated electrodes on each side and a 12 μ thick FEP Teflon film on the HMX side. The active area of this gauge is 3 mm by 3 mm. The side next to the HMX was coated with aluminum to eliminate any pyroelectric effects in the PVDF. Although gauge conditions were not exactly identical, they were as close as possible to being the same.

RESULTS

Experiments were performed at projectile velocities ranging from 0.15 to 0.7 km/s with corresponding stress inputs to the HMX samples between 0.1 and 0.8 GPa. At the lower input stresses, the compaction process dominated and the transmitted waves as measured by the back gauges had long rise times; the lowest input experiments were over 1μs. At the higher projectile velocities, evidence of reaction was apparent at both the front and back gauges. Figure 2 shows the particle velocity history plots obtained in the lowest input experiment (Shot 931). The projectile velocity was 0.158 km/s and the stress about 0.1 GPa. The transmitted gauge record has a risetime of over 3 μs with the front looking almost like an elastic precursor. This wave shape undoubtedly has to do with the dynamics of crushing and compaction of the HMX. The HMX was not compacted to 100% TMD in this experiment.

The Hugoniot data obtained from this and other experiments are presented in Table 1. Some of the experiment are paired (one shot at LANL and one at SNL) at the conditions where we were trying to make identical experiments. This turned out to be harder than expected because of a number of difficulties with the biggest one being making the two different guns produce the same projectile velocity on demand. At the lower projectile velocities, this was more difficult than expected. In any case we succeeded in getting some of the shot pairs very close in projectile velocity. The pairs are these: 912 and 2477, 913 and 2478, 928 and 2486, 929 and 2487, and 931 and 2489. For these pairs the Hugoniot point was obtained by taking the particle velocity from the LANL experiment and the stress from the SNL experiment.

Figure 3 shows particle velocity and stress waveforms obtained in two experiments (Shot 912 and Shot 2477) in which the projectile velocity was ≈ 0.29 km/s. In the front PVDF gauge measurement, there is a considerable overshoot in stress because of the Kel-F front plate (this overshoot was observed in all the front PVDF gauge measurements). The stress measurement in the HMX begins after this overshoot - about 40 ns into the record. Rounding at the top of both the front gauge waveforms results from the viscoelastic wave shaping that occurs in the shock as it moves through the Kel-F cell front. The back gauge waveforms show a very disperse wave with a risetime of ≈ 700 ns. This is due to the compaction process in the HMX that develops as the wave progresses through the sample. We do not know if the profile is steady but assume that

Shot No.	Lab	Projectile Vel. km/s	Measured u_p km/s	Measured P GPa	Calculated U_S km/s	Calculated ρ g/cm^3
931	LANL	0.158	0.132	0.087	0.532	1.651
2489	SNL	0.189				
912	LANL	0.288	0.23	0.20	0.701	1.844
2477	SNL	0.285				
942	LANL	0.406	0.29	0.35	0.973	1.767
2488	SNL	0.412				
929	LANL	0.509	0.37	0.48	1.046	1.919
2487	SNL	0.496				
928	LANL	0.599	0.43	0.65	1.219	1.916
2486	SNL	0.591				
913	LANL	0.696	0.50	0.90	1.45	1.890
2478	SNL	0.669				

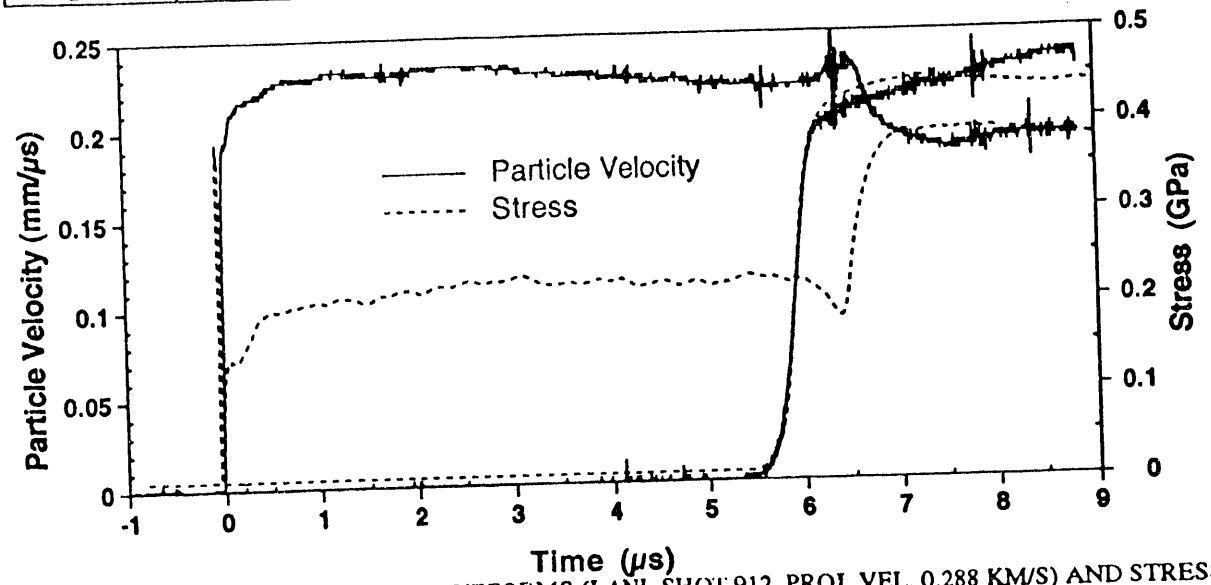

FIGURE 3. PARTICLE VELOCITY WAVEFORMS (LANL SHOT 912, PROJ. VEL. 0.288 KM/S) AND STRESS WAVEFORMS (SNL SHOT 2477, PROJ. VEL. 0.285 KM/S).

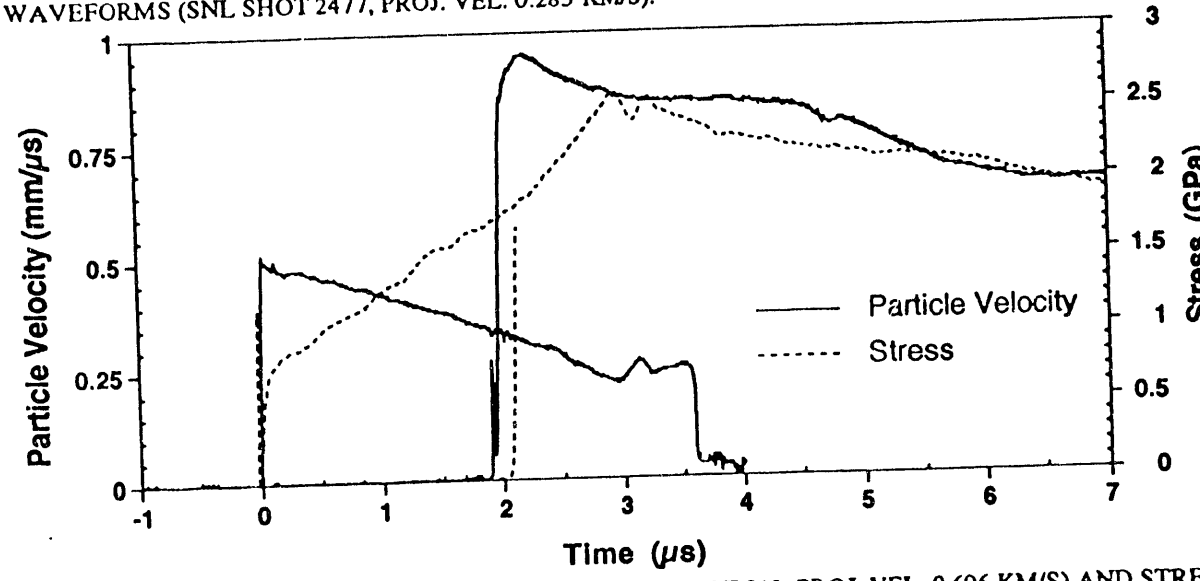

FIGURE 4. PARTICLE VELOCITY WAVEFORMS (LANL SHOT 913, PROJ. VEL. 0.696 KM/S) AND STRESS WAVEFORMS (SNL SHOT 2478, PROJ. VEL. 0.669 KM/S) .

it is not. There was apparently no reaction at this experimental condition.

Figure 4 gives the particle velocity and stress waveforms obtained in two experiments (Shot 913 and Shot 2478) in which the projectile velocity was ~ 0.68 km/s. In these experiments there is evidence of reaction in both the front and back gauge measurements. Reaction in the front gauge is manifested by a decrease in particle velocity (the reacting HMX is slowing down the cell front) and a corresponding increase in stress. The wave grows as it traverses the HMX sample because of reaction in the shock front so rather than the 0.5 km/s expected when a nonreactive wave interacts with the TPX back, a particle velocity of 0.35 km/s is measured. (The back PVDF gauge measurement was lost.) The risetime in the back particle velocity gauge was also considerably faster than in the lower input experiments (without reaction). However, it is still about 50 ns, longer than expected for a sharp shock. There is apparently competition between the reaction (trying to sharpen up the wave) and the compaction (trying to smear it out).

In this experiment the LANL projectile velocity was 4% higher than the SNL experiment. This is manifested in the data because the arrival time of the wave at the back PVDF gauge was longer than for the back particle velocity gauge. This gives an indication of the accuracy of the Hugoniot data from these experiments; it is on the order of 5% data in the worst case and somewhat better in the best case.

DISCUSSION

The Hugoniot data from the experiments in Table 1 were used to determine the adequacy of the EOS development described above. Table 2 lists the thermodynamic constants for the explosives HMX, HNS, and PETN. The latter two explosives have been included for comparison purposes. More information about the EOS and its application to HMX, HNS, PETN and other explosives can be found in Ref. 16. Brief comments about where the HMX constants were obtained, and how well they fit the data follow.

TABLE 1. THERMODYNAMIC CONSTANS

Explosive	ρ_0 g/cm^3	K_{T_0} Mbar	N	γ/V g/cm^3	C_v cm^2/μs^2/K
HMX	1.90	0.129	10.3	2.09	$1.05(10^{-5})$
HNS	1.74	0.146	3.5	2.82	$0.89(10^{-5})$
PETN	1.77	0.110	7.1	2.04	$1.00(10^{-5})$

K_{T_0} and N for HMX were obtained from fits to the hydrostatic pressure - volume data of Olinger, Roof and Cady.[17] γ and C_v are as reported in Ref. 17, as well. When these constants are used in the EOS given above, the curves shown in Figures 5 and 6 are produced. These constants, reproduce the 1.891 g/cm^3

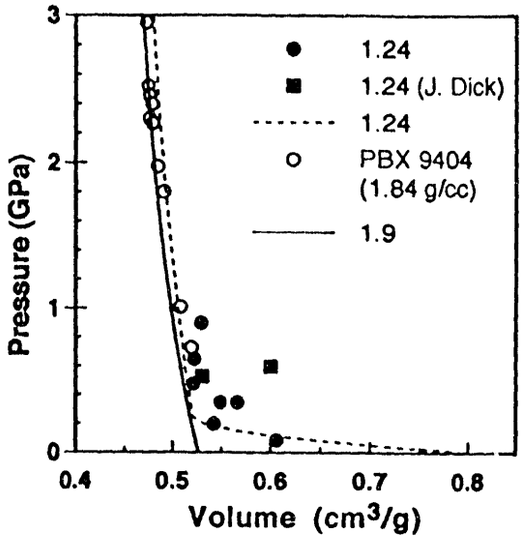

FIGURE 5. HUGONIOTS FOR HMX IN THE P-V PLANE.

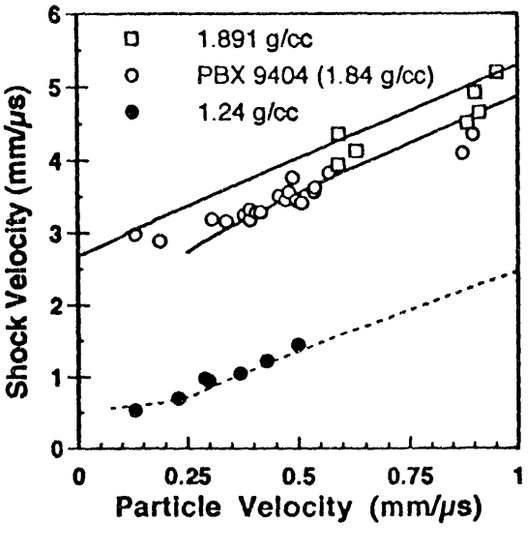

FIGURE 6. HUGONIOTS FOR HMX IN THE U_s-u_p PLANE.

and the PBX 9404 Hugoniot quite well up to pressures of about 10 GPa. Above 10 GPa, neither the PBX 9404, the 1.891 HMX, nor the single crystal HMX Hugoniots[19] are reproduced very well, possibly because of a phase transition in the HMX at a pressure near 10 GPa.[20] These constants, with P_s set equal to 0.25 GPa, nicely reproduce our Hugoniot measurements on 1.24 g/cc HMX as is shown in the figures. As is typical there is more scatter in the P-V than the U_S - u_p plane.

The risetimes of the transmitted waves are interesting in terms of indicating the competition between the dynamic compaction process (spreading out the wave) and the reaction process (steepening up the wave). Figure 7 shows the risetimes of the transmitted waves as a function of the input stress. At about 0.5 GPa the risetimes get to be below 100 ns, the minimum risetime for these experiments.

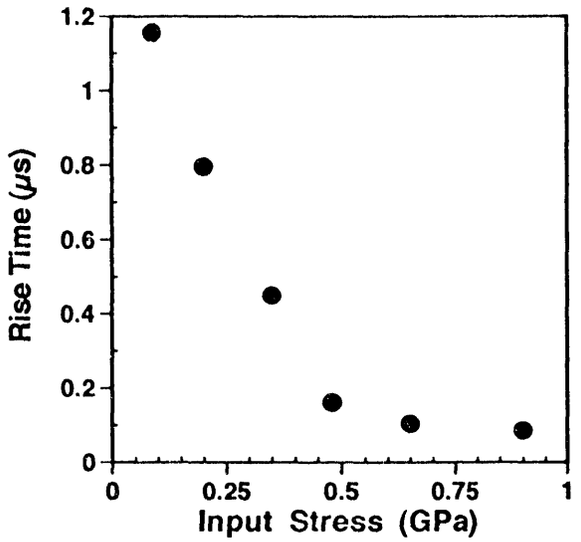

FIGURE 7. PLOT OF RISETIME FOR TRANSMITTED GAUGE WAVEFORMS VS. INPUT STRESS.

Using the particle velocity and stress data from the experiments, these two properties can be plotted against each other at the appropriate times in the stress vs. particle velocity plane. This plot can be superimposed on a Hugoniot cross plot to give some understanding of the processes occurring in the experiment. This has been done for the data shown in Fig. 3 , where there was no reaction, and is reported in Ref. 21. The case with reaction is discussed next.

The data shown in Fig. 4 are definitely in the regime where reaction is taking place. Using the front gauge data and plotting the stress vs. particle velocity results in the wiggly curve shown in Fig. 8. (The appropriate Hugoniots for Kel-F, low density HMX, and TPX are shown for reference purposes.) It starts somewhat low in stress, due to the viscoelastic effects in the Kel-F, but then moves along the backward facing Kel-F Hugoniot clear off the figure. In other words, the state at the front gauge as the reaction occurs moves up along the Kel-F Hugoniot because this is what it is in contact with. In this experiment the maximum stress at the front gauge was about 2.8 GPa at the end of the record. Ritchie[22] has calculated the BKW reaction product equation of state for 1.24 g/cm^3 HMX. Figure 8 has been expanded in Fig. 9 so that the BKW product isentrope and the porous HMX Hugoniot are shown. Using the product curve as the approximate end state for the reaction if it went to completion, it appears that the HMX has reacted to about the 40% point. This has taken place in about 3 μs, leading to an estimated global reaction rate of ≈ 0.13 μs^{-1} . Of course there are many assumptions in this rough analysis but it gives an indication of the order of the reaction rate that is occurring in the shocked porous HMX.

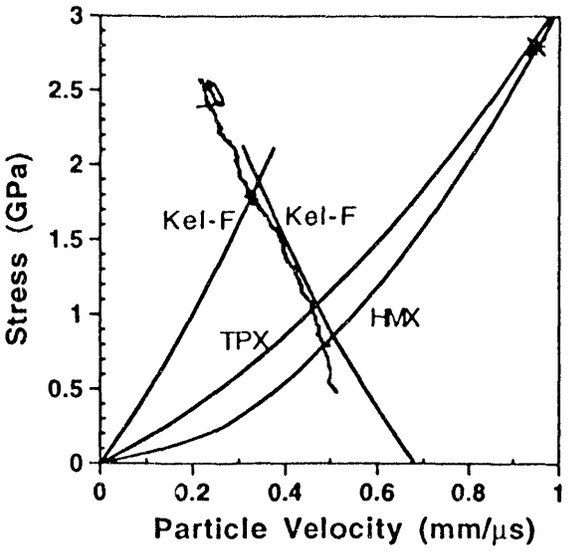

FIGURE 8. STRESS VS. PARTICLE VELOCITY PLOT OBTAINED USING THE DATA OF FIG. 4.

The back magnetic gauge had a maximum particle velocity of 0.95 km/s, which corresponds to a stress of 2.8 GPa on the unreacted HMX Hugoniot and a shock velocity of 2.4 km/s. An asterisk has been put on this point on the unreacted Hugoniot of Fig. 8. The average shock velocity through the sample was 1.96 km/s, considerably above the 1.36 km/s expected if there were no reaction. Considerable reaction is occurring in the shock front (as is normally the case for

this level. If the porous HMX were detonating, the detonation velocity would be 6.7 km/s so it is obvious that there is still a rather long buildup process to occur before detonation is achieved.

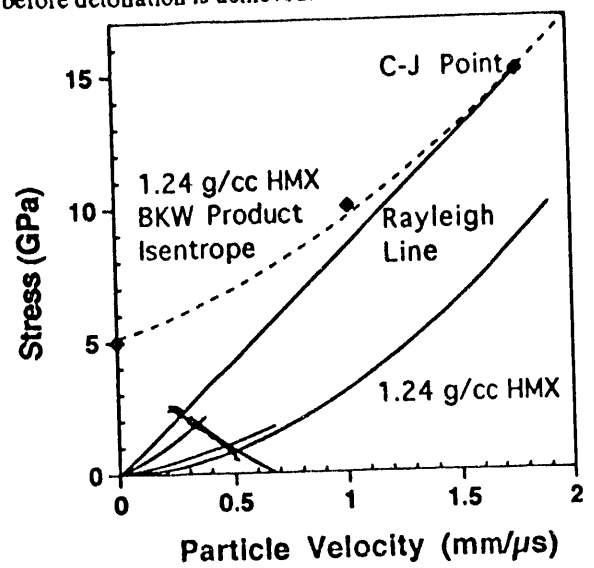

FIGURE 9. EXPANDED VIEW OF FIG. 8 SHOWING THE BKW PRODUCT ISENTROPE.

This set of experiments demonstrates the usefulness of making both stress and particle velocity measurements in near identical experiments. It is clear that to really understand the compaction and reaction processes in detail, computer modeling with accurate material, compaction, micromechanical, and reaction models will be required.

ACKNOWLEDGEMENTS

We would like to thank Ronald Rabie for useful discussions concerning the P-α model, and Jerry Dick and Jerry Wackerle for discussions concerning general properties of porous explosives.

REFERENCES

1. J. M. McAfee, B. W. Asay, A. W. Campbell, and J. B. Ramsay, Ninth Symposium (Intl.) on Detonation, Office of the Chief of Naval Research Report OCNR-113291-7, Arlington, VA (1989), p. 265.

2. G. E. Seay and L. B. Seely, Jr., J. Appl. Phys. 32, 1092 (1961).

3. M. W. Evans, B. O. Reese, L. B. Seely, and E. L. Lee, Fourth Symposium (Intl.) on Detonation, Office of Naval Research Report ACR-126, Washington, D.C.~ (1965), p. 359.

4. A. N. Dremin, S. A. Koldunov, and K. K. Shvedov, Comb. Expl. and Shock Waves 7 (1), 87 (1971).

5. I. E. Lindstrom, J. Appl. Phys. 41, 337 (1970).

6. J. J. Dick, Combustion and Flame 54, 121 (1983).

7. W. L. Elban and M. A. Charito, Powder Tech., 46, 181 (1986).

8. J. J. Dick, Combustion and Flame 69, 257 (1987).

9. F. Bauer, in Shock Waves in Condensed Matter, Y. M. Gupta, ed. (Plenum Press, New York, 1986), p. 483.

10. R. A. Graham, L. M. Lee, and F. Bauer, in Shock Waves in Condensed Matter 1987, S. C. Schmidt and N. C. Holmes, eds. (North-Holland, Amsterdam 1988), p. 619.

11. J. O. Erkman and D. J. Edwards, Sixth Symposium (Intl.) on Detonation, Office of Naval Research Report ACR-221, Arlington, VA (1976), p. 766.

12. S. A. Sheffield, D. E. Mitchell, and D. B. Hayes, Sixth Symposium (Intl.) on Detonation, Office of Naval Research Report ACR-221, Arlington, VA (1976), p. 748.

13. R.E. Setchell and P.A. Taylor, J. Energetic Mat. 6, 157 (1988).

14. W. Hermann, J. Appl. Phys. 40, 2490 (1969).

15. M.M. Carroll and A.C. Holt, J. Appl. Phys. 45, 3864 (1974).

16. R. L. Gustavsen and S. A. Sheffield, presented at the joint AIRAPT/APS Conference, June 28 - July 2, 1993, Colorado Springs, CO.

17 B. Olinger, B. Roof, and H. Cady in "Symposium H.D.P. (Commissariat a l'Energie Atomique)", 1978. pg. 3.

18 LASL Shock Hugoniot Data, S.P. Marsh Ed. U. of California Press, Berkeley, (1980) pg. 596.

19. Ref. 18, pg. 595.

20. J.J. Dick, J. Energetic Mat. 1, 275 (1983).

21. S. A. Sheffield, R. L. Gustavsen, R. R. Alcon, R. A. Graham, and M. U. Anderson, presented at the joint AIRAPT/APS Conference, June 28 - July 2, 1993, Colorado Springs, CO.

22. J. P. Ritchie, Los Alamos National Lab., Group T-14, private communication.

this level. If the porous HMX were detonating, the detonation velocity would be 6.7 km/s so it is obvious that there is still a rather long buildup process to occur before detonation is achieved.

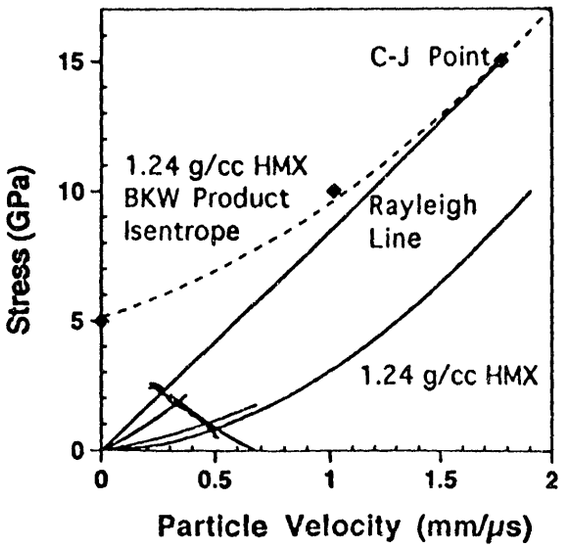

FIGURE 9. EXPANDED VIEW OF FIG. 8 SHOWING THE BKW PRODUCT ISENTROPE.

This set of experiments demonstrates the usefulness of making both stress and particle velocity measurements in near identical experiments. It is clear that to really understand the compaction and reaction processes in detail, computer modeling with accurate material, compaction, micromechanical, and reaction models will be required.

ACKNOWLEDGEMENTS

We would like to thank Ronald Rabie for useful discussions concerning the P-α model, and Jerry Dick and Jerry Wackerle for discussions concerning general properties of porous explosives.

REFERENCES

1. J. M. McAfee, B. W. Asay, A. W. Campbell, and J. B. Ramsay, Ninth Symposium (Intl.) on Detonation, Office of the Chief of Naval Research Report OCNR-113291-7, Arlington, VA (1989), p. 265.

2. G. E. Seay and L. B. Seely, Jr., J. Appl. Phys. 32, 1092 (1961).

3. M. W. Evans, B. O. Reese, L. B. Seely, and E. L. Lee, Fourth Symposium (Intl.) on Detonation, Office of Naval Research Report ACR-126, Washington, D.C.- (1965), p. 359.

4. A. N. Dremin, S. A. Koldunov, and K. K. Shvedov, Comb. Expl. and Shock Waves 7 (1), 87 (1971).

5. I. E. Lindstrom, J. Appl. Phys. 41, 337 (1970).

6. J. J. Dick, Combustion and Flame 54, 121 (1983).

7. W. L. Elban and M. A. Charito, Powder Tech., 46, 181 (1986).

8. J. J. Dick, Combustion and Flame 69, 257 (1987).

9. F. Bauer, in Shock Waves in Condensed Matter, Y. M. Gupta, ed. (Plenum Press, New York, 1986), p. 483.

10. R. A. Graham, L. M. Lee, and F. Bauer, in Shock Waves in Condensed Matter 1987, S. C. Schmidt and N. C. Holmes, eds. (North-Holland, Amsterdam 1988), p. 619.

11. J. O. Erkman and D. J. Edwards, Sixth Symposium (Intl.) on Detonation, Office of Naval Research Report ACR-221, Arlington, VA (1976), p. 766.

12. S. A. Sheffield, D. E. Mitchell, and D. B. Hayes, Sixth Symposium (Intl.) on Detonation, Office of Naval Research Report ACP.-221, Arlington, VA (1976), p. 748.

13. R.E. Setchell and P.A. Taylor, J. Energetic Mat. 6, 157 (1988).

14. W. Hermann, J. Appl. Phys. 40, 2490 (1969).

15. M.M. Carroll and A.C. Holt, J. Appl. Phys. 45, 3864 (1974).

16. R. L. Gustavsen and S. A. Sheffield, presented at the joint AIRAPT/APS Conference, June 28 - July 2, 1993, Colorado Springs, CO.

17 B. Olinger, B. Roof, and H. Cady in "Symposium H.D.P. (Commissariat a l'Energie Atomique)", 1978. pg. 3.

18 LASL Shock Hugoniot Data, S.P. Marsh Ed. U. of California Press, Berkeley, (1980) pg. 596.

19. Ref. 18, pg. 595.

20. J.J. Dick, J. Energetic Mat. 1, 275 (1983).

21. S. A. Sheffield, R. L. Gustavsen, R. R. Alcon, R. A. Graham, and M. U. Anderson, presented at the joint AIRAPT/APS Conference, June 28 - July 2, 1993, Colorado Springs, CO.

22. J. P. Ritchie, Los Alamos National Lab., Group T-14, private communication.

DATE

FILMED

11/9/93

END